EurJIC
European Journal of Inorganic Chemistry

A Journal of ChemPubSoc Europe

Accepted Article

Title: Zwitterionic mixed-carbene coinage metal complexes: Synthesis, structures and photophysical studies

Authors: Florian Chotard, Alexander S. Romanov, David L. Hughes, Mikko Linnolahti, and Manfred Bochmann

To be cited as: *Eur. J. Inorg. Chem.* 10.1002/ejic.201900573

Link to VoR: http://dx.doi.org/10.1002/ejic.201900573

WILEY-VCH

10.1002/ejic.201900573

WILEY-VCH

Zwitterionic Mixed-Carbene Coinage Metal Complexes: Synthesis, Structures and Photophysical Studies

Florian Chotard,[a] Alexander S. Romanov,[a] David L. Hughes,[a] Mikko Linnolahti*[b] and Manfred Bochmann*[a]

"EuCheMS Inorganic Chemistry Celebrates the Anniversary of the Periodic Table of Elements"

Abstract: A series of three zwitterionic mixed-ligand bis(carbene) complexes of copper (**1**), silver (**2**) and gold (**3**) have been synthesized, based on a combination of ethyl-substituted cyclic (alkyl)(amino)carbene (^{Et2}CAAC) and an anionic methyl-malonate-derived N-heterocyclic carbene (*malo*NHC). The crystal structures confirm the linear two-coordinate geometry without close intermolecular contacts. The compounds show blue-white phosphorescence consistent with a wide HOMO-LUMO energy gap (2.87–3.07 eV) estimated by cyclic voltammetry. The excited state lifetimes of crystalline powders decrease in the series Cu > Ag > Au, from 400 µs for copper **1** to 50 µs for the gold complex **3**. DFT calculations indicate a large change in the transition dipole moment on excitation, of up to 16 D.

Introduction

Gold complexes of *N*-heterocyclic carbene (NHC) ligands displaying photoluminescence (PL) were first reported by Lin in 1999.[1] Since this first highlight, photoluminescent NHC complexes of coinage metals have attracted much attention,[2,3] since such compounds are interesting candidates for optoelectronic applications, in particular as emitter materials in organic light-emitting diodes (OLEDs).[4]

We showed recently that two-coordinate carbene complexes of copper(I), silver(I) and gold(I) incorporating cyclic (alkyl)(amino)carbene (CAAC) ligands show strong photo-luminescence.[5-7] CAAC ligands are based on 5-ring system where the carbene-C atom is stabilised by only one N atom,[8] as opposed to the more commonly employed imidazolylidene-type NHC carbenes with two N donors. CAAC ligands are not only strong σ-donors but, by virtue of the empty p-orbital on the carbene-carbon, are also good π-acceptors.[9] Even simple halide complexes (CAAC)MX (M = Cu, Au; X = Cl, Br, I) are highly photoemissive; for example, in the solid state (CAAC)CuCl complexes show a photoluminescence quantum yield (PLQY) of up to 96%.[5] Substitution of the halide ligand e.g. by aryloxides or arylamides provides a facile route to a wide range of photoemissive compounds.[6] Of these, the introduction of diarylamides and of carbazolates as anions proved particularly effective and gave rise to so-called carbene-metal-amide (CMA) class of photoemitters.[10-15] These CMAs allowed the fabrication of OLEDs with near-100% internal and up to 27% external quantum efficiency (EQE) by solution[10] and vapour deposition[12,13] methods. (CAAC)M-amide complexes are highly polar,[11-15] and DFT calculations demonstrated the strong charge-transfer character of the excitation process.[10,16-18]

An alternative to halide or amide ligands would be the use of anionic carbenes, based on imidazolylidene-type NHC carbenes which possess on their backbone a moiety bearing an anionic charge while being π-conjugated to the NHC moiety.[19] This family of ligands has been intensively studied, and some of them were used to stabilise group 11 metal ions.[20-22] Anionic 6-ring NHC ligands based on a malonate unit (*malo*NHC*)*, have also been developed and coordinated to silver[23] and to gold halide and phosphine complexes,[24] including reports on copper halide and copper bis(carbene) complexes.[25] To the best of our knowledge, zwitterionic carbene ligands have not been used in the context of photoluminescence studies.[19] We report here the synthesis, structures and properties of a series of zwitterionic copper, silver and gold mixed-carbene complexes incorporating both a CAAC and a *malo*NHC ligand..

Results and Discussion

The precursor (*malo*NHC)H was synthesized according to a literature procedure.[25] The corresponding anionic carbene can be generated *in situ* or isolated in an intermediate step in the presence of a strong base [$KN(SiMe_3)_2$ or *n*BuLi]. Complexes **1** – **3** were prepared in moderate to good yields by mixing the anionic carbene with (^{Et2}CAAC)MCl[6,7] (M = Cu, Ag, Au) in THF at room temperature for 1 h (Scheme 1). These compounds show good solubility in THF and dichloromethane and are moderately soluble in acetonitrile, toluene and diethyl ether but insoluble in alkanes. They are isolated as white solids which are stable to air for prolonged periods of time.

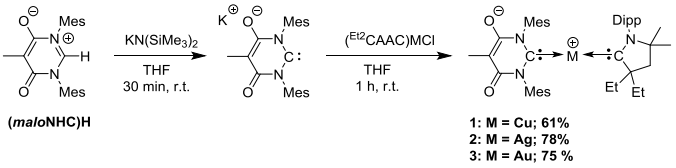

Scheme 1. Synthesis of complexes **1–3** (Mes = 2,4,6-trimethylphenyl, Dipp = 2,6-di*iso*propylphenyl).

[a] Dr F. Chotard, Dr A. S. Romanov, Dr D. L. Hughes, Prof. Dr M. Bochmann, School of Chemistry, University of East Anglia, Norwich NR4 7TJ, UK; e-mail m.bochmann@uea.ac.uk
[b] Prof. Dr M. Linnolahti, Department of Chemistry, University of Eastern Finland, Joensuu Campus, FI-80101 Joensuu, Finland; e-mail mikko.linnolahti@uef.fi

Supporting information for this article is given via a link at the end of the document.

The complexes have been characterised by NMR spectroscopy, elemental analysis and X-ray diffraction. The products present two distinctive downfield ^{13}C NMR signals for the two carbene-C atoms, one at δ = 251.4–259.2 ppm for the CAAC ligand and 193.2–198.8 ppm for the *malo*NHC ligand. Complex **2** exhibits the two ^{13}C(carbene) NMR signals at δ_C 259.2 and 193.8 ppm as two doublets due to coupling to ^{107}Ag and ^{109}Ag silver isotopes, with coupling constants similar to those found for cationic bis(carbene) silver complexes.[7]

Single crystals of the complexes were obtained either by slow evaporation of benzene (for **1**) or by CH_2Cl_2/hexane layering (for **2** and **3**). The crystal structures of **1** – **3** are essentially identical; the structure of **1** is shown in Figure 1 (see ESI for details of **2** and **3**). Selected bond lengths and angles are collected in Table 1. All three complexes display almost linear coordination geometries around the metal centre. The M–$C_{carbene}$ bond lengths are slightly longer for the *malo*NHC than for the CAAC ligand ($\Delta_{malo\text{NHC/CAAC}}$ = 0.009–0.014 Å). Both carbene ligands are almost co-planar, with torsion angles (defined as the angle between the *malo*NHC N2–C23–N3 and CAAC C2–C1–N1 planes) of 4.60 – 20.63°. There are no significant close intermolecular contacts between the molecules.

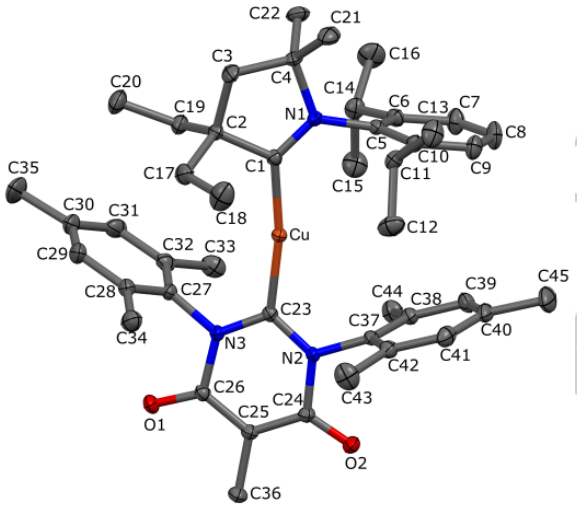

Figure 1. Crystal structures of complexes **1**. For selected geometric parameters of **1**, **2** and **3** see Table 1.

Electrochemistry

Cyclic voltammetry (CV) was used to analyse the redox behaviour of complexes **1** – **3** in THF solution, using [*n*Bu$_4$N][PF$_6$] as supporting electrolyte (Table 2). The three complexes present similar behaviour; they undergo quasi-reversible reduction and irreversible oxidation processes (see Supporting Information Figures S2–S4). The nature of the metal has a significant impact on the reduction potentials. The reduction potential of the silver derivative **2** ($E_{1/2}$ = –2.81 V) is 0.08 V and 0.26 V more negative than the potentials of the copper **1** and gold **3** analogues, respectively. The gold compound **3** presents the highest oxidation potential (E_p = +0.58 V), 0.09 V more positive than the copper and silver congeners. The estimated HOMO/LUMO energy levels were identified based on reduction and oxidation *onset* potentials.[26] The HOMO–LUMO gap of the silver complex **2** ($\Delta E_{HOMO/LUMO}$ = 3.07 eV) is larger by 0.10 and 0.22 eV, respectively, than that of the copper and gold complexes.

Table 1. Selected bond lengths (Å) and angles (°) of complexes **1–3**

	M–C1	M–C23	C1–M–C23 (°)	N_2–C_{23}–N_3 (°)	C_2–C_1–N_1 (°)	Malo/CAAC, (°)
1	1.9275(17)	1.9403(17)	170.22(7)	115.12(15)	108.64(14)	20.63
2	2.113(2)	2.122(2)	170.93(7)	115.39(17)	109.26(17)	14.26
3	2.041(4)	2.055(4)	173.87(14)	115.9(3)	109.5(3)	4.60

Table 2. Formal electrode potentials (peak position E_p for irreversible and $E_{1/2}$ for quasi-reversible processes [V] vs. ferrocene Fc/Fc$^+$), onset potentials (E [V] vs. Fc/Fc$^+$), peak to peak separation for quasi-reversible processes (ΔE_p in mV), $E_{HOMO/LUMO}$ [eV] and band gap values (ΔE, eV) for the redox changes exhibited by complexes **1**–**3**.[a]

	Reduction			Oxidation			
	$E_{1/2}$	$E_{onset\ red}$	E_{LUMO}	E_p	$E_{onset\ ox}$	E_{HOMO}	ΔE
1	–2.73	–2.63	–2.76	+0.49	+0.34	–5.73	2.97
2	–2.81	–2.73	–2.66	+0.49	+0.34	–5.73	3.07
3	–2.55	–2.47	–2.92	+0.58	+0.38	–5.77	2.85

[a] Cyclic voltammograms recorded in THF solution (1.4 mM) at 0.1 Vs^{-1} using a glassy carbon electrode, with [*n*Bu$_4$N][PF$_6$] (0.13 M) as supporting electrolyte.

Computational Studies

Density functional theory (DFT) calculations show that the highest occupied molecular orbital (HOMO) is almost entirely based on the *malo*NHC ligand, with only minimal metal contribution (1.9% in the case of gold). Whereas in (CAAC)metal carbazolates the lowest unoccupied molecular orbital (LUMO) is centred on the CAAC ligand,[10,13] in **1** – **3** the LUMO encompasses the C-atoms of both the CAAC and the *malo*NHC ligands (Figure 2). The LUMO is almost entirely located on the p-orbitals of the carbene-C atoms, while the metal contribution to the LUMO is again low (6.5% for Au). This suggests that excitation involves mainly ligand-to-ligand charge transfer from the anionic carbene to CAAC. The dipole changes on going from the S_0 to the S_1 state are smaller than was found for carbene metal amides; for example, on excitation the dipole of the gold complex **3** reduces from 16.3 D to 1.4 D (in S_1@S_0 geometry), but, unlike the situation for (^{Ad}CAAC)Au(carbazolate),[10] it does not change direction. Dipole moment changes are important in the excitation and emission processes of these compounds.[17] The calculations reproduce the order of emission energies which decrease in the sequence Ag > Cu > Au (see ESI, Table S1).

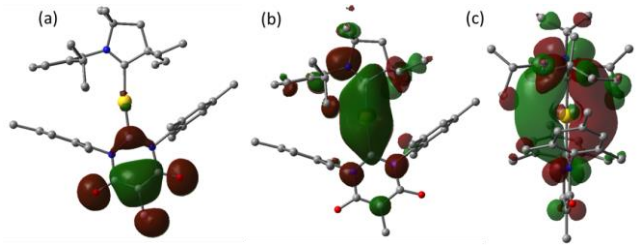

Figure 2. HOMO (a) and LUMO in top (b) and side (c) view of the gold complex **3** [isovalue = 0.02 (electron/bohr^3)$^{1/2}$; red (green), positive (negative) sign of wave function].

Photophysical properties

UV-visible absorption spectra of complexes **1–3** were measured in THF solution at room temperature (Figure 3 and SI, Table S2). Two high energy absorption bands at ca. 230 and 264 nm can be ascribed to π–π* ligand-centred (LC) transitions for the maloNHC and CAAC carbene ligands, respectively, and line with previous reports on related CAAC compounds.[5,6,7] All complexes show a broad energy absorption band (λ = 320–420 nm) with molar extinction coefficients in the range of 2900–3000 M^{-1}cm^{-1}. Notably for complex **1**, this absorption band is structured, which would indicate an overlap of several metal-to-ligand charge transfer (MLCT: *malo*NHC→Cu and CAAC→Cu) and ligand-to-ligand charge transfer (LLCT) transitions. This CT band shows a red-shifts in the order Cu (346 nm) < Ag (353 nm) < Au (384 nm).

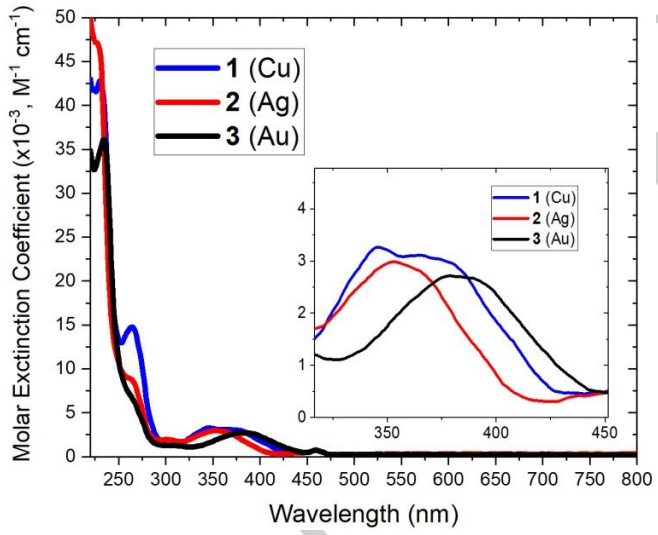

Figure 3. UV–visible absorption spectra of complexes **1–3** in THF solution at room temperature.

Complexes **1–3** are blue-white phosphors in the solid state, in toluene solution, and in polystyrene (PS) films (Figure 4). Photophysical data are collected in Table 3. The full-width-half-maximum (FWHM) values for heteroleptic **1** – **3** are twice as broad as those of homoleptic cationic biscarbene complexes (L_2Cu^+ where L = CAAC[6] or diamidocarbene DAC[3k]). The largest FWHM value was observed for silver **2** (5100 cm^{-1}), followed by copper **1** (4300 cm^{-1}) and gold **3** (4100 cm^{-1}). Such broadness of the emission profiles for **1** – **3** suggests that several emission processes are likely to contribute to the total emission. This is clearly seen in the solid-state PL spectrum of the gold complex **3** (Figure 4a) which shows a prominent shoulder at ca. 500 nm. Compared with homoleptic biscarbene copper complexes,[3k,6] the PLQY values are low, *ca.* 2 – 3% for **1** and **3**. The excited state lifetime measurements (Figure 4) of the compounds in the solid state show a bi-exponential decay. The short component of 3.7–4.4 µs likely originates from charge transfer from CAAC to the metal, similar to the previously reported value of 7 µs for the homoleptic CAAC complex $[Cu(^{Et2}CAAC)_2]^+$.[6] The presence of the second component can be explained by an emission process involving charge transfer from the *malo*NHC carbene to the metal. This component is very sensitive to the nature of the metal atom and decreases down the triad in the sequence 401 µs (Cu, **1**) > 353 µs (Ag, **2**) >> 49.9 µs (Au, **3**). The decrease in the excited state lifetimes follows the increase of the spin-orbit coupling coefficients from copper to gold. The long excited state lifetimes for **1** – **3** are commensurate with phosphorescence.

We examined the photoluminescence of complexes **1** – **3** in PS films (loading 5 weight-%). When excited with 360 nm UV-light, all complexes emit blue light, similar to the powdered solids (Figure 4b). The excited state lifetimes show bi-exponential decay but the long component is significantly shorter that in the neat solids, in the range of 9 – 22 µs (Table 1). Toluene solutions of **1** – **3** are poorly emissive.

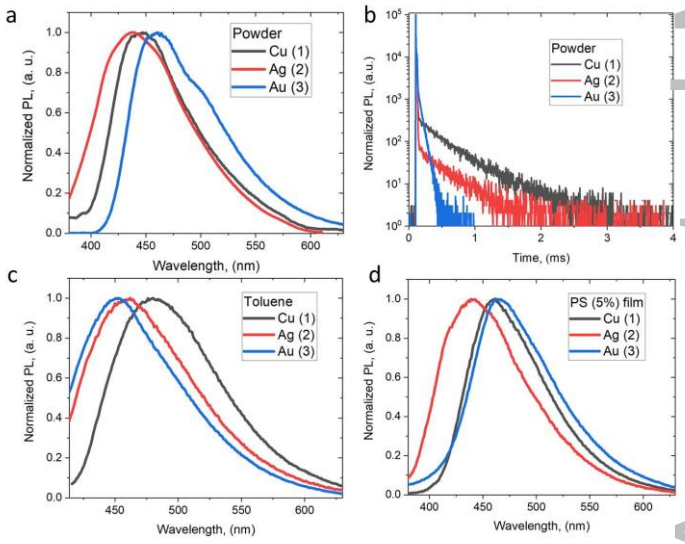

Figure 4. Emission spectra of complexes **1** – **3** as microcrystalline powders (a), in toluene solution (c), and in polystyrene films (doping level 5 weight-%) (d); and emission decay kinetics of solid powders of **1–3** (b).

Table 3. PL data for **1** – **3** at 298 K for crystalline powders, toluene solutions and PS films (dopant level 5 weight-%).

	1			2			3		
	Powder	Toluene	PS[a]	Powder	Toluene	PS[a]	Powder	Toluene	PS[a]
λ_{em} (nm)	455	480	460	438	459	440	461	453	464
τ(µs)	3.7 and 401	–	1.4 and 9	4 and 353	–	3.8 and 11.6	4.4 and 49.9	–	1.5 and 22
Φ(%, 300K; N_2)	1.7	–	2.3	<0.1	–	0.3	2.7	–	2.9
FWHM (cm^{-1})	4300	4243	3801	5100	4730	4693	4100	4625	3958

[a] Polystyrene films (5% by weight) were drop-cast from 10 mg/mL toluene solutions on a quartz substrate and evaporated under reduced pressure in a nitrogen-filled glove box chamber.

Conclusions

The reaction of *malo*NHC anions with (CAAC)metal halide complexes affords stable copper, silver and gold zwitterionic mixed-carbene complexes, (CAAC)M(*malo*NHC). These compounds show a coplanar structure similar to (carbene)metal amides (CMAs). The HOMO and LUMO energies strongly resemble those of their CMA congeners; however, calculations show that the LUMO is delocalised across the carbene-C atoms of both CAAC and *malo*NHC carbenes, which results in significant overlap between HOMO and LUMO. All complexes show high transition dipole moments of up to 16 D but no inversion in the dipole direction on excitation. All three complexes have a relatively broad emission profile which results in blue-white luminescence. The solid-state excited state lifetimes decrease significantly in the series Cu > Ag > Au, from 400 to 50 µs, in line with the increase in spin-orbit coupling coefficients. These compounds based on a combination of different carbene ligands extend the principle of donor-acceptor light emitting molecules from the now well-established carbene-metal-amides to alternative emitters based on a linear coordination geometry.

Experimental Section

All reactions were carried out under an atmosphere of argon using conventional Schlenk techniques. CH_2Cl_2, diethyl ether, THF, and hexane were freshly distilled from appropriate drying agents. (*malo*NHC)H and corresponding carbene (*malo*NHC)Li[25], (^{Et2}CAAC)CuCl,[6] (^{Et2}CAAC)AgCl[7] and (^{Et2}CAAC)AuCl[6] were synthesised according to literature procedures. The identity and purity (≥95%) of the compounds were established using elemental analyses, multinuclear NMR spectroscopy and X-ray diffraction analysis. CHN elemental analyses were performed at the London Metropolitan University. NMR spectra [^{1}H, ^{13}C{^{1}H}] were recorded on a Bruker Avance DPX-300 MHz spectrometer. All acquisitions were performed at 300 K. Chemical shifts are quoted in parts per million (δ) relative to TMS. For ^{1}H and ^{13}C{^{1}H} spectra, values were determined by using solvent residual signal ($CHDCl_2$ in CD_2Cl_2) as internal standard. The coupling constants (*J*) are reported in Hertz (Hz). Assignment of ^{1}H and ^{13}C signals was established through the use of 2D experiments (COSY, NOESY, HMQC, and HMBC). Photoluminescence measurements were recorded on a Fluorolog Horiba Jobin Yvon spectrofluorometer with a solids mount attachment where appropriate. Photoluminescence quantum yield were recorded using an integrating sphere on an Edinburgh Instruments FS5 spectrofluorometer under a nitrogen atmosphere. The emission decays were collected on an Edinburgh Instruments FS5 spectrofluorometer using the 5 W microsecond Xe flashlamp with a repetition rate of 100 Hz (excitation at 360 nm and emission at 490 nm).

Preparation of 1. An oven-dried Schlenk flask was charged with (*malo*NHC)H (1 eq., 0.3 mmol, 109 mg) and $KN(SiMe_3)_2$ (1.1 eq., 1.6 THF adduct, 0.33 mmol, 104 mg). THF (6 mL) was added and the mixture was stirred 30 min at r.t. while a white precipitate progressively appeared. (^{Et2}CAAC)CuCl (0.3 mmol, 124 mg) was added and the mixture was further stirred 1 h at room temperature. The volatiles were evaporated, and the white residue was washed with diethyl ether (3 x 10 mL). The residue was extracted into dichloromethane (2 x 10 mL). The filtrate was concentrated and the resulting solid was washed with hexane (10 mL) to give the product as an off-white solid (91 mg, 61 %). ^{1}H NMR (300 MHz, CD_2Cl_2): δ (ppm) = 7.39 (t, $^3J_{HH}$ = 7.8 Hz, 1H, *p*-Dipp), 7.07 (d, $^3J_{HH}$ = 7.8 Hz, 2H, *m*-Dipp), 6.80 (s, 4H, *m*-Mes), 2.53 (hept, $^3J_{HH}$ = 6.8 Hz, 2H, CH *i*Pr), 2.35 (s, 6H, 2 x CH_3 *p*-Mes), 1.96 (s, 12H, 4 x CH_3 *o*-Mes), 1.77 (s, 3H, CH_3 Malo overlapping with CH_2 CAAC), 1.75 (s, 2H, CH_2 CAAC overlapping with CH_3 Malo), 1.20 (s, 6H, $C(CH_3)_2$ CAAC), 1.16 (d, $^3J_{HH}$ = 6.8 Hz, 6H, 2 x CH_3 a *i*Pr), 0.90 (d, $^3J_{HH}$ = 6.8 Hz, 6H, 2 x CH_3 b *i*Pr overlapping with CH_2 Et), 0.96 – 0.80 (m, 4H, 2 x CH_2 Et), 0.72 (t, $^3J_{HH}$ = 7.2 Hz, 6H, 2 x CH_3 Et). ^{13}C{^{1}H} NMR (75 MHz, CD_2Cl_2): δ (ppm) = 252.0 (C, carbene CAAC), 193.2 (C, carbene Malo), 161.4 (C, C=O), 144.2 (C, *o*-Dipp), 138.7 (C, *i*-Mes), 137.8 (C, *p*-Mes), 136.1 (C, *o*-Mes), 134.7 (C, *i*-Dipp), 129.84 (CH, *p*-Dipp), 129.78 (CH, *m*-Mes), 124.7 (CH, *m*-Dipp), 92.8 (C, $\underline{C}CH_3$ Malo), 82.5 (C, $\underline{C}(CH_3)_2$ CAAC), 63.5 (C, CEt_2), 40.2 (CH_2, CAAC), 29.8 (CH_2, Et), 29.5 (CH_3, $C(\underline{C}H_3)_2$), 29.1 (CH, *i*Pr), 28.0 (CH_3, CH_3 a *i*Pr), 22.4 (CH_3, CH_3 b *i*Pr), 21.6 (CH_3, *p*-Mes), 18.5 (CH_3, *o*-Mes), 9.8 (CH_3, Et), 9.3 (CH_3, Malo). Elemental analysis calcd for $C_{45}H_{60}CuN_3O_2$: C, 73.18; H, 8.19; N, 5.69; found: C, 72.89; H, 8.21; N, 5.74.

Preparation of 2. Following the procedure described for **1**, the complex was made from (^{Et2}CAAC)AgCl (1 eq., 0.3 mmol, 137 mg) as a white solid (183 mg, 78 %). ^{1}H NMR (300 MHz, CD_2Cl_2): δ (ppm) = 7.40 (t, $^3J_{HH}$ = 7.8 Hz, 1H, *p*-Dipp), 7.09 (d, $^3J_{HH}$ = 7.8 Hz, 2H, *m*-Dipp), 6.80 (s, 4H, *m*-Mes), 2.52 (hept, $^3J_{HH}$ = 6. 8 Hz, 2H, CH *i*Pr), 2.34 (s, 6H, 2 x CH_3 *p*-Mes), 1.96 (s, 12H, 4 x CH_3 *o*-Mes), 1.79 (s, 3H, CH_3 Malo overlapping with CH_2 CAAC), 1.77 (s, 2H, CH_2 CAAC overlapping with CH_3 Malo), 1.21 (s, 6H, $C(CH_3)_2$ CAAC), 1.18 (d, $^3J_{HH}$ = 6.8 Hz, 6H, 2 x CH_3 a *i*Pr), 1.14 – 1.01 (m, 2H, $C\underline{H}_aH_b$ Et), 0.88 (d, $^3J_{HH}$ = 6.8 Hz, 6H, 2 x CH_3 b *i*Pr overlapping with $CH_a\underline{H}_b$ Et), 0.90 – 0.78 (m, 2H, 2 x $CH_a\underline{H}_b$ Et), 0.73 (t, $^3J_{HH}$ = 7.2 Hz, 6H, 2 x CH_3 Et). ^{13}C{^{1}H} NMR (75 MHz, CD_2Cl_2): δ (ppm) = 259.2 (2 x d, $^1J_{C\text{-}109Ag}$ = 190.4 Hz, $^1J_{C\text{-}107Ag}$ = 164.9 Hz, C, carbene CAAC), 193.8 (2 x d, $^1J_{C\text{-}109Ag}$ = 205.1 Hz, $^1J_{C\text{-}107Ag}$ = 177.5 Hz, C, carbene Malo), 161.4 (d, $^3J_{CAg}$ = 6.1 Hz, C, C=O), 144.5 (s, C, *o*-Dipp), 140.0 (d, $^3J_{CAg}$ = 2.5 Hz, C, *i*-Mes), 137.6 (s, C, *p*-Mes), 135.5 (s, C, *o*-Mes), 134.7 (d, $^3J_{CAg}$ = 2.7 Hz, C, *i*-Dipp), 129.9 (s, CH, *p*-Dipp), 129.6 (s, CH, *m*-Mes), 124.6 (s, CH, *m*-Dipp), 92.0 (s, C, $\underline{C}CH_3$ Malo), 83.6 (d, $^3J_{CAg}$ = 9.4 Hz, C, $\underline{C}(CH_3)_2$ CAAC), 63.5 (d, $^3J_{CAg}$ = 7.9 Hz, C, CEt_2), 40.1 (d, $^3J_{CAg}$ = 3.6 Hz, CH_2, CAAC), 30.3 (s, CH_2, Et), 29.5 (s, CH_3, $C(\underline{C}H_3)_2$),

29.1 (s, CH, *i*Pr), 27.8 (s, CH_3, CH_3 a *i*Pr), 22.3 (s, CH_3, CH_3 b *i*Pr), 21.6 (s, CH_3, *p*-Mes), 18.2 (s, CH_3, *o*-Mes), 9.5 (s, CH_3, Et), 9.3 (s, CH_3, Malo). Elemental analysis calcd for $C_{45}H_{60}AgN_3O_2$: C, 69.04; H, 7.73; N, 5.37; found: C, 68.96; H, 7.89; N, 5.47.

Preparation of 3. In an oven dried Schlenk flask, Li(*malo*NHC) (THF adduct, 43.9 mg, 0.1 mmol) and (^{Et2}CAAC)AuCl (54.6 mg, 0.1 mmol,) were mixed in THF (5 mL) and stirred 1 h at room temperature. The volatiles were evaporated. The residue was washed with diethyl ether (2 x 5 mL) and extracted with CH_2Cl_2 (2 x 5 mL). The filtrate was evaporated to give the product as an off-white solid (65 mg, 75 %). ^{1}H NMR (300 MHz, CD_2Cl_2): δ (ppm) = 7.40 (t, $^3J_{HH}$ = 7.8 Hz, 1H, *p*-Dipp), 7.07 (d, $^3J_{HH}$ = 7.8 Hz, 2H, *m*-Dipp), 6.79 (s, 4H, *m*-Mes), 2.48 (hept, $^3J_{HH}$ = 6.9 Hz, 2H, CH *i*Pr), 2.34 (s, 6H, 2 x CH_3 *p*-Mes), 1.94 (s, 12H, 4 x CH_3 *o*-Mes), 1.82 (s, 2H, CH_2 CAAC),1.77 (s, 3H, CH_3 Malo), 1.21 (s, 6H, $C(CH_3)_2$ CAAC), 1.16 (d, $^3J_{HH}$ = 6.6 Hz, 6H, 2 x CH_3 a *i*Pr), 1.12 – 1.02 (m, 2H, CH_aH_b Et overlapping with CH_3 b *i*Pr), 1.00 (d, $^3J_{HH}$ = 6.8 Hz, 6H, 2 x CH_3 b *i*Pr), 0.99 – 0.88 (m, 2H, 2 x CH_aH_b Et overlapping with CH_3 b *i*Pr), 0.75 (t, $^3J_{HH}$ = 7.2 Hz, 6H, 2 x CH_3 Et). $^{13}C\{^1H\}$ NMR (75 MHz, CD_2Cl_2): δ (ppm) = 251.4 (C, carbene CAAC), 198.8 (C, carbene Malo), 161.3 (C, C=O), 144.5 (C, *o*-Dipp), 138.5 (C, *i*-Mes), 137.7 (C, *p*-Mes), 135.8 (C, *o*-Mes), 134.0 (C, *i*-Dipp), 130.0 (CH, *p*-Dipp), 129.5 (CH, *m*-Mes), 124.8 (CH, *m*-Dipp), 92.3 (C, CCH_3 Malo), 82.3 (C, $C(CH_3)_2$ CAAC), 63.6 (C, CEt_2), 40.6 (CH_2, CAAC), 30.8 (CH_2, Et), 29.5 (CH_3, $C(CH_3)_2$), 29.2 (CH, *i*Pr), 27.6 (CH_3, CH_3 a *i*Pr), 22.7 (CH_3, CH_3 b *i*Pr), 21.6 (CH_3, *p*-Mes), 18.2 (CH_3, *o*-Mes), 9.5 (CH_3, Et), 9.4 (CH_3, Malo). Elemental analysis calcd for $C_{45}H_{60}AuN_3O_2$: C, 61.99; H, 6.94; N, 4.82; found: C, 61.85; H, 6.72; N, 4.83.

Computational details

The S_0 ground states of complexes **1**-**3** were studied by DFT using the global hybrid MN15 functional with especially good performance for noncovalent interactions and excitation energies.[27] The def2-TZVP basis set[28,29] was employed with relativistic effective core potential of 28 and 60 electrons for description of the core electrons of Ag and Au, respectively.[30] Excited S_1 and T_1 states were studied by time-dependent DFT (TD-DFT) using the same method / basis set.[31] The calculations initially suffered from triplet instability problems typical for TD-DFT, but were overcome by switching to the Tamm-Dancoff approximation (TDA-DFT) as recommended.[32] All calculations were carried out by Gaussian 16.[33]

X-Ray Crystallography.

Crystals of **1**–**3** suitable for X-ray diffraction study were obtained by slow evaporation of benzene (for **1**) or by layering technique from CH_2Cl_2/hexane (for **2** and **3**). Crystals were mounted in oil on glass fibre and fixed on the diffractometer in a cold nitrogen stream. Data were collected using an Oxford Diffraction Xcalibur-3/Sapphire3-CCD diffractometer with graphite monochromated Mo K_α radiation (λ = 0.71073 Å) at 140 K. Data were processed using the CrystAlisPro-CCD and –RED software.[34] The structure was solved by the intrinsic phasing routines and refined by full-matrix least-squares methods against F^2 in an anisotropic (for non-hydrogen atoms) approximation. All hydrogen atom positions were refined in isotropic approximation in a "riding" model with the $U_{iso}(H)$ parameters equal to 1.2 $U_{eq}(C_i)$ or, for methyl groups equal to 1.5 $U_{eq}(C_{ii})$, where $U(C_i)$ and $U(C_{ii})$ are respectively the equivalent thermal parameters of the carbon atoms to which the corresponding H atoms are bonded. All calculations were performed using the SHELX software.[35,36] The data have been deposited with the Cambridge Crystallographic Data Centre: CCDC 1918028 (**1**), CCDC 1918029 (**2**), CCDC 1918027 (**3**).

Electrochemistry.

Electrochemical experiments were performed using an Autolab PGSTAT 302N computer-controlled potentiostat. Cyclic voltammetry (CV) was performed using a three-electrode configuration consisting of either a glassy carbon macrodisk working electrode (GCE) (diameter of 3 mm; BASi, Indiana, USA) combined with a Pt wire counter electrode (99.99 %; GoodFellow, Cambridge, UK) and an Ag wire pseudoreference electrode (99.99 %; GoodFellow, Cambridge, UK). The GCE was polished between experiments using alumina slurry (0.3 µm), rinsed in distilled water and subjected to brief sonication to remove any adhering alumina microparticles. The metal electrodes were then dried in an oven at 100 °C to remove residual traces of water, the GCE was left to air dry and residual traces of water were removed under vacuum. The Ag wire pseudoreference electrodes were calibrated to the ferrocene/ferrocenium couple in THF at the end of each run to allow for any drift in potential, following IUPAC recommendations.[37] All electrochemical measurements were performed at ambient temperatures under an inert argon atmosphere in THF containing the complex under study (1.4 m*M*) and supporting electrolyte [n-Bu_4N][PF_6] (0.13 *M*). Data were recorded with Autolab NOVA software (v. 1.11).

.

Acknowledgements

This work was supported by the European Research Council, the Royal Society. M. B. is an ERC Advanced Investigator Award holder (grant no. 338944-GOCAT). The computations were made possible by use of the Finnish Grid Infrastructure resources (urn:nbn:fi:research-infras-2016072533). A. S. R. acknowledges support from the Royal Society (grant nos. URF\R1\180288 and RGF\EA\181008).

Keywords: Copper, Silver, Gold, Carbene, Luminescence, Coordination Complex

[1] H. M. J. Wang, C. Y. L. Chen, I. J. B. Lin, *Organometallics* **1999**, *18*, 1216 –1223.

[2] Reviews: a) J. C. Y. Lin, R. T. W. Huang, C. S. Lee, A. Bhattacharyya, W. S. Hwang, I. J. B. Lin, *Chem. Rev.* **2009**, *109*, 3561–3598; b) R. Visbal, M. C. Gimeno, *Chem. Soc. Rev.* **2014**, *43*, 3551 – 3574; c) For an overview of related structures see also R. C. Evans, P. Douglas, C. J. Winscom, *Coord. Chem. Rev*. **2006**, *250*, 2093–2126; d) H. Yersin, R. Czerwieniec, M. Z. Shafikov, A. F. Suleymanova, *ChemPhysChem* **2017**, *18*, 3508 – 3535; e) Y. R. Liu, S.-C. Yiu, C.-L. Ho, W.-Y. Wong, *Coord. Chem. Rev*. **2018**, *375*, 514–557; f) C. Bizzarri, F. Hundemer, J. Busch, S. Bräse, *Polyhedron* **2018**, *140*, 51–66; g) C. Bizzarri, E. Spuling, D. M. Knoll, D. Volz, S. Bräse, *Coord. Chem. Rev*. **2018**, *373*, 49–82.

[3] a) P. J. Barnard, L. E. Wedlock, M. V. Baker, S. J. Berners-Price, D. A. Joyce, B. W. Skelton, J. H. Steer, *Angew. Chem. Int. Ed*. **2006**, *45*, 5966 –5970; b) K. Matsumoto, N. Matsumoto, A. Ishii, T. Tsukuda, M. Hasegawa and T. Tsubomura, *Dalton Trans.*, **2009**, 6795–6801; c) M. C. Gimeno, A. Laguna, R. Visbal, *Organometallics* **2012**, *31*, 7146−7157; d) V. A. Krylova, P. I. Djurovich, J. W. Aronson, R. Haiges, M. T. Whited, and M. E. Thompson, *Organometallics* **2012**, 31, 7983−7993; e) A. Gómez-Suárez, D. J. Nelson, D. G. Thompson, D. B. Cordes, D. Graham, A. M. Z. Slawin, S. P. Nolan, *Beilstein J. Org. Chem.* **2013**, *9,* 2216–2223; f) E. Y.-H. Hong, H.-L. Wong, V. W.-W.

Yam, *Chem. Eur. J.* **2015**, *21*, 5732 –5735; g) V. A. Krylova, P. I. Djurovich, B. L. Conley, R. Haiges, M. T. Whited, T. J. Williams and M. E. Thompson, *Chem. Commun.,* **2014**, 50, 7176—7179; h) R. Marion, F. Sguerra, F. Di Meo, E. Sauvageot, J.-F. Lohier, R. Daniellou, J.-L. Renaud, M. Linares, M. Hamel, S. Gaillard, *Inorg. Chem*. **2014**, *53*, 9181−9191; i) B. Hupp, C. Schiller, C. Lenczyk, M. Stanoppi, K. Edkins, A. Lorbach, A. Steffen, *Inorg. Chem*. **2017**, *56*, 8996−9008; j) M. Gernert, U. Meller, M. Haehnel, J. Pflaum, A. Steffen, *Chem. Eur. J*. **2017**, *23*, 2206 – 2216; k) S. Y. Shi, L. R. Collins, M. F. Mahon, P. I. Djurovich, M. E. Thompson, M. K. Whittlesey, *Dalton Trans*. **2017**, *46*, 745–752; l) R. Hamze, R. Jazzar, M. Soleilhavoup, P. I. Djurovich, G. Bertrand, M. E. Thompson, *Chem. Commun.,* **2017**, *53*, 9008—9011; m) Q. Liu, M. Xie, X. Y. Chang, S. Cao, C. Zou, W.-Fu Fu, C.-M. Che, Y. Chen, W. Lu, *Angew. Chem. Int. Ed*. **2018**, *57*, 6279 –6283.

[4] H. Yersin (ed.), *Highly Efficient OLEDs*, Wiley-VCH, Weinheim 2019, ISBN: 978-3-527-33900-6.

[5] (a) A. S. Romanov, D. Di, L. Yang, J. Fernandez-Cestau, C. R. Becker, C. E. James, B. Zhu, M. Linnolahti, D. Credgington and M. Bochmann, *Chem. Commun.* **2016**, *52*, 6379–6382 and **2018**, *54*, 3672.

[6] A. S. Romanov, C. R. Becker, C. E. James, D. Di, D. Credgington, M. Linnolahti, M. Bochmann, *Chem. Eur. J.* **2017**, *23*, 4625 – 4637.

[7] A. S. Romanov and M. Bochmann, *J. Organomet. Chem.* **2017**, *847*, 114–120.

[8] a) V. Lavallo, Y. Canac, C.Präsang, B. Donnadieu, G. Bertrand, *Angew. Chem. Int. Ed*. **2005**, *44*, 5705 – 5709; b) R. Jazzar, R. D. Dewhurst, J. B. Bourg, B. Donnadieu, Y. Canac, G. Bertrand, *Angew. Chem. Int. Ed.* **2007**, *46*, 2899 – 2902; c) M. Melaimi, R. Jazzar, M. Soleilhavoup, G. Bertrand, *Angew. Chem. Int. Ed*. **2017**, *56*, 10046 – 10068; d) M. Soleilhavoup, G. Bertrand, *Acc. Chem. Res*. **2015**, *48*, 256−266, and cited refs.

[9] a) O. Back, M. Henry-Ellinger, C. D. Martin, D. Martin, G. Bertrand, *Angew. Chem. Int. Ed*. **2013**, 52, 2939 – 2943; b) K. C. Mondal, S. Roy, B. Maity, D. Koley, H. W. Roesky, *Inorg. Chem*. **2016**, *55*, 163−169.; c) A. Liske, K. Verlinden, H. Buhl, K. Schaper, C. Ganter, *Organometallics* **2013**, *32*, 5269-5272; d) K. Verlinden, H. Buhl, W. Frank, C. Ganter, *Eur. J. Inorg. Chem*. **2015**, 2416-2425.

[10] D. Di, A. S. Romanov, L. Yang, J. M. Richter, J. P. H. Rivett, S. Jones, T. H. Thomas, M. Abdi Jalebi, R. H. Friend, M. Linnolahti, M. Bochmann and D. Credgington, *Science* **2017**, *356*, 159–163.

[11] C. R. Hall, A. S. Romanov, M. Bochmann, S. R. Meech, *J. Phys. Chem. Lett*. **2018**, *9*, 5873–5876.

[12] P. J. Conaghan, S. M. Menke, A. S. Romanov, S. T. E. Jones, A. J. Pearson, E. W. Evans, M. Bochmann, N. C. Greenham, D. Credgington, *Adv. Mater.* **2018**, *30*, 1802285.

[13] A. S. Romanov, S. T. E. Jones, L. Yang, P. J. Conaghan, D. Di, M. Linnolahti, D. Credgington, M. Bochmann, *Adv. Optical Mater.* **2018**, *6*, 1801347.

[14] R. Hamze, J. L. Peltier, D. Sylvinson, M. C. Jung, J. Cardenas, R. Haiges, M. Soleilhavoup, R. Jazzar, P. I. Djurovich, G. Bertrand, and M. E. Thompson, *Science* **2019**, *363*, 601–606.

[15] S. Shi, M. C. Jung, C. Coburn, A. Tadle, D. Sylvinson M. R., P. I. Djurovich, S. R. Forrest, and M. E. Thompson, *J. Am. Chem. Soc*. **2019**, *141*, 3576−3588.

[16] S. Thompson, J. Eng, T. J. Penfold, *J. Chem. Phys*. **2018**, *149*, 014304.

[17] J. Föller, C.M. Marian, *J. Phys. Chem. Lett.*, **2017**, *8*, 5643–5647.

[18] E. J. Taffet, Y. Olivier, F. Lam, D. Beljonne, G. D. Scholes, *J. Phys. Chem. Lett*. **2018**, *9*, 1620−1626.

[19] a) A. Nasr, A. Winkler, M. Tamm, *Coord. Chem. Rev.* **2016**, *316*, 68–124; b) M. Ruamps, N. Lugan, V. César, *Eur. J. Inorg. Chem*. **2017**, 4167-4173.

[20] L. Benhamou, N. Vujkovic, V. César, H. Gornitzka, N. Lugan, G. Lavigne, *Organometallics* **2010**, *29*, 2616–2630.

[21] S. K. Hashmi, C. Lothschütz, K. Graf, T. Häffner, A. Schuster, F. Rominger, *Adv. Synth. Catal.*, **2011**, *353*, 1407–1412.

[22] V. César, V. Mallardo, A. Nano, G. Dahm, N. Lugan, G. Lavigne, S. Bellemin-Laponnaz, *Chem. Commun.* **2015**, *51*, 5271–5274.

[23] V. César, N. Lugan, G. Lavigne, *J. Am. Chem. Soc.* **2008**, *130*, 11286–11287.

[24] S. Bastin, C. Barthes, N. Lugan, G. Lavigne, V. César, *Eur. J. Inorg. Chem.* **2015**, 2216–2221.

[25] V. César, C. Barthes, Y. C. Farré, S. V. Cuisiat, B. Y. Vacher, R. Brousses, N. Lugan, G. Lavigne, *Dalton Trans.* **2013**, *42*, 7373-7385.

[26] C. M. Cardona, W. Li, A. E. Kaifer, D. Stockdale, G. C. Bazan, *Adv. Mater.*, 2011, 23, 2367–2371.

[27] H. S. Yu, X. He, S.L. Li, D. G. Truhlar, *Chem. Sci*. **2016**, *7*, 5032–5051.

[28] F. Weigend, M. Häser, H. Patzelt, R. Ahlrichs, *Chem. Phys. Lett.* **1998**, *294*, 143–152.

[29] F. Weigend, R. Ahlrichs, *Phys. Chem. Chem. Phys.* **2005**, *7*, 3297–3305.

[30] D. Andrae, U. Haeussermann, M. Dolg, H. Stoll, H. Preuss, *Theor. Chim. Acta* **1990**, *77*, 123–141.

[31] F. Furche, D. Rappoport, Density functional methods for excited states: equilibrium structure and electronic spectra. In: *Computational Photochemistry*; M. Olivuccim, Ed.; Elsevier: Amsterdam, 2005; pp. 93–128.

[32] M. J. G. Peach, D. J. Tozer, *J. Phys. Chem. A* **2012**, *116*, 9783–9789.

[33] Gaussian 16, Revision A.03, M. J. Frisch, G. W. Trucks, H. B. Schlegel, G. E. Scuseria, M. A. Robb, J. R. Cheeseman, G. Scalmani, V. Barone, G. A. Petersson, H. Nakatsuji, X. Li, M. Caricato, A. V. Marenich, J. Bloino, B. G. Janesko, R. Gomperts, B. Mennucci, H. P. Hratchian, J. V. Ortiz, A. F. Izmaylov, J. L. Sonnenberg, D. Williams-Young, F. Ding, F. Lipparini, F. Egidi, J. Goings, B. Peng, A. Petrone, T. Henderson, D. Ranasinghe, V. G. Zakrzewski, J. Gao, N. Rega, G. Zheng, W. Liang, M. Hada, M. Ehara, K. Toyota, R. Fukuda, J. Hasegawa, M. Ishida, T. Nakajima, Y. Honda, O. Kitao, H. Nakai, T. Vreven, K. Throssell, J. A. Montgomery, Jr., J. E. Peralta, F. Ogliaro, M. J. Bearpark, J. J. Heyd, E. N. Brothers, K. N. Kudin, V. N. Staroverov, T. A. Keith, R. Kobayashi, J. Normand, K. Raghavachari, A P. Rendell, J. C. Burant, S. S. Iyengar, J. Tomasi, M. Cossi, J.M. Millam, M. Klene, C. Adamo, R. Cammi, J. W. Ochterski, R. L. Martin, K. Morokuma, O. Farkas, J.B. Foresman, D. J. Fox, Gaussian, Inc., Wallingford CT, 2016.

[34] *Programs CrysAlisPro*, Oxford Diffraction Ltd., Abingdon, UK (2010).

[35] G.M. Sheldrick, Program for crystal structure determination (SHELXT), **2015**, *A71*, 3-8.

[36] G.M. Sheldrick, Crystal structure refinement with SHELXL, *Acta Cryst.* **2008**, *A64*, 112 and **2015**, *C71*, 3-8 (Open Access).

[37] G. Gritzner, J. Kůta, *Electrochim. Acta* **1984**, *29*, 869–873.